*Original Article*

Microbial Biosystems 10(2) (2025) 2025.370215
10.21608/mb.2025.370215.1283

Contents lists available at Egyptian Knowledge Bank
Microbial Biosystems
Journal homepage: http://mb.journals.ekb.eg/

# In Silico comparative analysis of type III secretion system effector proteins of *Pseudomonas aeruginosa* as agents of *Acanthamoeba* spp. killing

**Charlemagne G. Sumperos[1], Julia Aliyah C. Zalzos[1], Ed Lois O. Ubalde[1], Marielle M. Trinidad[1], An Gheline Ubina[1], Josiah T. Valentin[1], Revielmer Alfred Tuguinay[1], Mary Rose F. Lirio[1*]**

*Department of Medical Technology, Institute of Health Sciences and Nursing, Far Eastern University – Manila, Nicanor Reyes St., Sampaloc, Manila, Metro Manila, Philippines.*

**ARTICLE INFO**

***Article history***
Received 21 March 2025
Received revised 16 April 2025
Accepted 17 May 2025
Available online 1 June 2025

***Corresponding Editors***
Gomez, C.
Parcon, C.

***Keywords***
Amoebae,
host-pathogen interaction,
molecular docking,
phospholipase.

**ABSTRACT**

The Type III Secretion System (T3SS) of Pseudomonas aeruginosa plays a critical role in its pathogenicity by delivering effector proteins directly into host cells. This study conducted an in silico comparative analysis of four T3SS effector proteins (ExoS, ExoT, ExoU, and ExoY) to elucidate their molecular mechanisms in targeting *Acanthamoeba* spp., a genus of free-living amoebae with significant public health implications. Using bioinformatic tools, we examined the molecular structures, physicochemical properties, and cytotoxic mechanisms of these effectors. Structural characterization revealed distinct functional domains: ExoS and ExoT share overlapping activities but differ in their mechanisms, with ExoS disrupting cellular processes via ADP-ribosyltransferase activity and ExoT impairing phagocytosis through its GTPase-activating protein domain. ExoU's phospholipase activity leads to membrane disruption and necrotic cell death, while ExoY interferes with cytoskeletal integrity through adenylate cyclase activity, increasing intracellular cAMP levels. Molecular docking analyses demonstrated stable binding interactions between these effectors and *Acanthamoeba castellanii*, highlighting their specific cytotoxic pathways. These findings provided insights into the pathogenesis of *P. aeruginosa* and offer a foundation for the development of novel therapeutic strategies against *Acanthamoeba* infections.

**Published by Arab Society for Fungal Conservation**

## Introduction

*Acanthamoeba* spp. is a well-recognized member of the free-living amoebas that is widely distributed in any environmental niche. Its life cycle consists of two stages: an active, feeding trophozoite and a dormant, non-feeding cyst that forms under unfavorable conditions (Wang et al., 2023). It is the causative agent of granulomatous amebic encephalitis (GAE), a fatal central nervous system infection that primarily affects immunocompromised individuals, including those undergoing chemotherapy, antibiotic treatment, or those with HIV/AIDS (Scruggs et al., 2024). Additionally, *Acanthamoeba* can cause *Acanthamoeba* keratitis, a rare but serious eye infection commonly observed in contact lens wearers (Chomicz et al., 2024).

Although infections are caused by the trophozoite stage, the cyst form is highly resistant to anti-*Acanthamoeba* drugs and biocides, making treatment

***Corresponding author Email address**: mlirio@feu.edu.ph (Mary Rose Lirio)

challenging (So-Young et al., 2022). As a result, the inhibition of encystation may be a more effective strategy in treating *Acanthamoeba* infections. Despite the potentially severe consequences of these infections, research on free-living amoeba in the Philippines remains limited. This may be due to the relatively low number of reported cases, with only 12 documented instances of *Acanthamoeba* keratitis and two cases of GAE in the country as of 2022 (Milanez et al., 2022).

*Pseudomonas aeruginosa*, on the other hand, is a gram-negative opportunistic pathogen that grows optimal at 25° C to 37° C. Initially thought to be a true pathogen of plants, the bacteria has become one of the most resistant pathogens related to nosocomial infections, having enzymes and mechanisms that help its ability to resist quaternary disinfectants, aminoglycosides, carbapenems, cephalosporins, and ureidopenicillins (Labovská, 2021). Its ability to successfully infect and easily adapt to unfavorable environments is due to the bacterium's virulence factors including lipopolysaccharide (LPS), outer membrane proteins, and secretion systems such as T6SS-associated flagella, T4SS-associated pili, and, most importantly, multi-toxin components Type III Secretion System (T3SS) (Qin et al., 2022).

The T3SS effector proteins (ExoS, ExoT, ExoU, and exoY) of *Pseudomonas aeruginosa* is a vital virulence factor for the pathogenicity of a bacteria to cause harm as it allows the direct transfer of toxic proteins into the host's cytoplasm (Horna & Ruiz, 2021). Aside from inhibiting the immune system, it can also program cell death in immune cells such as neutrophils and macrophages. By avoiding phagocytosis, *Pseudomonas aeruginosa* successfully establishes itself during infection, resulting in important clinical issues, particularly in immunocompromised people. According to the study of Leong et. al (2022), the T3SS protein effector can alleviate the lethality of *Acanthamoeba* spp. by modifying its pathogenicity once inhabited.

Treating well-established *Acanthamoeba* keratitis remains challenging due to delayed diagnosis and cyst resistance, which prolongs infections and leads to frequent relapses. Current drug therapies, such as diamidines and biguanides, are more effective against cysts but are cytotoxic to corneal cells, posing additional risks to patients (Büchele et al., 2023). Given these limitations, alternative therapeutic approaches are needed. One promising target is the Type III Secretion System (T3SS) protein effectors of *Pseudomonas aeruginosa*, which have the potential to weaken *Acanthamoeba* virulence. Since *Acanthamoeba* is widely present in water sources, water purification challenges in the Philippines may further contribute to the risk of amoebic infections (Castro & Obusan, 2023). Therefore, this study aims to investigate the inhibitory potential of T3SS protein effectors from *P. aeruginosa* in reducing *Acanthamoeba* virulence, particularly in vulnerable populations such as immunocompromised individuals. The findings of this research may provide valuable insights into developing novel anti-amoebic therapies while also informing public health strategies for preventing infections.

## Materials and Methods

### *Retrieval of Amino Sequences and Proteomics*

Amino acid sequences were retrieved for the target proteins: the T3SS effector proteins of *Pseudomonas aeruginosa*, specifically ExoS (WP_320524392.1), ExoT (WP_039027028.1), ExoU (WP_031686411.1), and ExoY (WP_319179002.1) and the cell wall anchor domain containing protein of *Acanthamoeba castellanii* str. Neff (XP_004338735.1) were primarily obtained from the National Center for Biotechnology Information (NCBI) database. In addition, UniProt protein database was utilized for cross-verification of the target proteins. UniProt's advanced and extensive protein database was employed to scrutinize and verify the integrity of the selected proteins, enhancing the reliability and accuracy of the *in silico* analysis.

### Multiple Sequence Alignment and Phylogenetic Tree Analysis

Once the amino acid sequences were retrieved, the sequences were aligned using BLASTp which compares the input protein sequences against those in the NCBI database to identify regions of similarity across different sequences (Nirjhon 2023). These identified similarities are important for determining the functional and structural relationships between proteins. The alignment results highlighted key regions essential for the proteins' activities during bacterial infection processes. Moreover, ClustalOmega was employed to align multiple protein sequences simultaneously to compare several sequences and identify conserved regions and genetic relationships among them.

### Physiochemical Profiling

The primary structure analysis for the protein sequences was performed using ProtParam which examined the primary structure sequence of each protein and calculated various properties using biochemical rules, coefficients, and constants. This enabled researchers to obtain essential information and characteristics without conducting laboratory experiments such as number of amino acids, chemical formula, molecular weight, total number of atoms,

theoretical pH, estimated half-life, instability index, aliphatic index, and isoelectric points.

For the secondary structure, SOPMA and PSIPRED was utilized. SOPMA was employed to predict the secondary structure of the T3SS effector proteins, specifically ExoS, ExoT, ExoU, and ExoY by aligning amino acid sequences to identify conserved structural elements, including alpha-helices, beta-sheets, and random coils. To validate and enhance the predictions, PSIPRED was utilized as a supplementary tool. By incorporating data from homologous sequences, PSIPRED identified patterns that may not have been evident from direct sequence alignment alone and to further analyze the secondary structural elements of the T3SS effector proteins.

As for constructing the tertiary structure of each protein, SWISS-MODEL, I-TASSER, and Phyre2 was used. SWISS-MODEL was responsible for generating 3D protein structure homology models based on the provided template sequence. I-TASSER was utilized as a tool to cross-validate the generated models by producing multiple possible 3D conformations. Phyre2 was used for cross-checking the homology models generated that added confidence to the in silico analysis by cross-referencing the models generated by the other bioinformatic tools to the models that this tool produced.

### Structural Quality assessment and refinement

Once the models were generated, they were subjected to verification using the PROCHECK and WHATCHECK servers available on the SAVES v.6.1 website. Once the models had been validated, the next step was refining the 3D models using the GalaxyWEB server which detected unfavorable regions caused by inaccuracies in the tertiary structure, such as misaligned loops or poorly executed secondary structures.

### Molecular Docking and Visualization of Protein

The refined models were subjected to ClusPro 2.0 through its server in deepening the understanding of protein-to-protein interaction of the T3SS effector proteins of *P. aeruginosa* and the cell wall anchor domain-containing protein of *A. castellanii* str. Neff. Moreover, this process produced a new protein that provided insights on its interaction with its environment. The receptor molecule was the cell wall anchor domain-containing protein of *Acanthamoeba castellanii* str. Neff., and the T3SS effector proteins as the ligand protein were then uploaded to the tool. The results were seen and was downloaded after careful evaluation using the cluster scores provided on the website. To visualize the models, the researcher employed a software called PyMol. This aided in the examination of the new potential interactions of the protein with its environment by visualizing the conformational changes (i.e., hydrogen bonds, hydrophobicity, and electrostatic interactions), which provided insights on its new function and interactions with its environment.

## Results

### Analysis of the Primary Structure

As presented in Table 1, the effector proteins of the Type III Secretion System (T3SS) exhibit varying sequence lengths: ExoS (453 amino acids), ExoT (457 amino acids), ExoU (687 amino acids), and ExoY (378 amino acids). Among these, ExoU had the highest molecular weight (~73.9 kDa), whereas the other three proteins were all below 50 kDa. The theoretical isoelectric point (pI) values indicated that all four effector proteins were slightly acidic, with ExoY exhibiting the highest pI among them. Notably, the *Acanthamoeba* cell wall was also found to be acidic.

In terms of aromatic amino acid composition, ExoU contained the highest abundance of these residues, allowing it to absorb the most ultraviolet (UV) light at 280 nm. Conversely, the *Acanthamoeba* cell wall had the lowest abundance of aromatic residues and demonstrated a highly flexible, hydrophilic structure, as reflected by its extinction coefficient of 18,910. Despite variations in molecular properties, all proteins, including the *Acanthamoeba* cell wall, were found to be stable across different biological conditions. However, based on the instability index, ExoS (25.77) and ExoY (35.32) were identified as the most stable among the effector proteins.

ExoS was also determined to be the most hydrophobic protein, exhibiting greater stability in specific environmental conditions due to its high aliphatic index (94.41). ExoT and ExoU displayed similar aliphatic indices, while the *Acanthamoeba* cell wall shared the exact same aliphatic index as ExoS. Additionally, the Grand Average of Hydropathicity (GRAVY) analysis revealed that both ExoS and the *Acanthamoeba* cell wall were moderately hydrophilic, each with a GRAVY value of 0.076. In contrast, ExoT (-0.313), ExoU (-0.239), and ExoY (-0.419) were more hydrophilic in nature.

**Table 1** Physicochemical Properties of the T3SS Effector proteins and the Cell Wall Anchor Domain Containing Protein of *Acanthamoeba castellanii* str. Neff using ProtParam Tool.

| Parameter | T3SS Effector Proteins of *P. aeruginosa* | | | | Cell wall anchor domain (*A. castellanii* str. Neff) |
|---|---|---|---|---|---|
| | ExoS | ExoT | ExoU | ExoY | |
| Number of amino acids | 453 | 457 | 687 | 378 | 254 |
| Molecular weight (Da) | 48,316 | 48,513 | 73,947 | 41,701 | 28,038 |
| Theoretical pI | 5.71 | 5.66 | 5.72 | 6.61 | 4.94 |
| Extinction coefficient | 19,940 | 19,940 | 29,450 | 23,170 | 18,910 |
| Estimated half-life | 30 hours (mammalian reticulocytes, in vitro)<br>>20 hours (yeast, in vivo)<br>>10 hours (*E. coli*, in vivo) | | | | |
| Instability index | 25.77 | 43.01 | 48.74 | 35.32 | 25.77 |
| Aliphatic index | 94.41 | 90.02 | 91.80 | 76.14 | 94.41 |
| GRAVY | 0.076 | -0.313 | -0.239 | -0.419 | 0.076 |

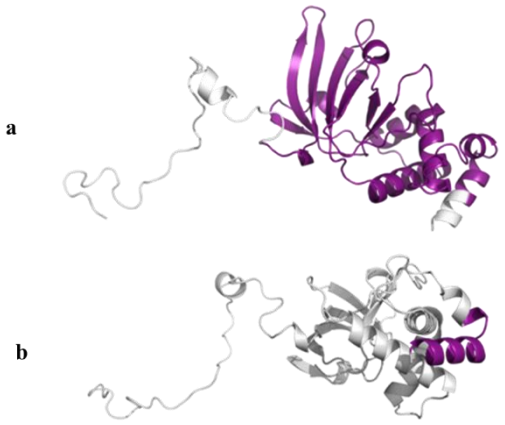


**Fig 1.** ExoS Important Regions (A) ADP Ribosyltransferase (ADPr) domain in purple (B) catalytic site for ExoS ADP-ribosyltransferase activity in purple

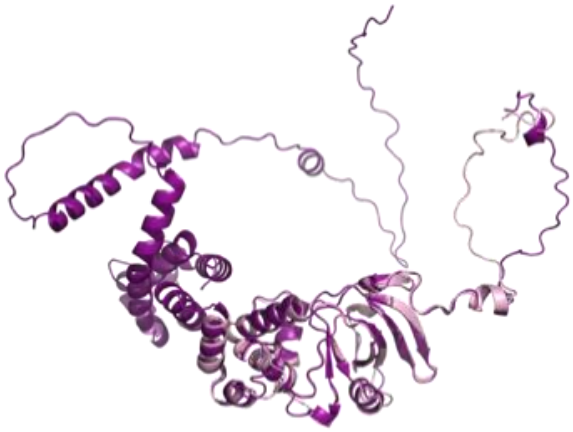

**Fig 3.** Superimposition of the ADPr Domain of ExoS (light pink) and ExoT (purple)

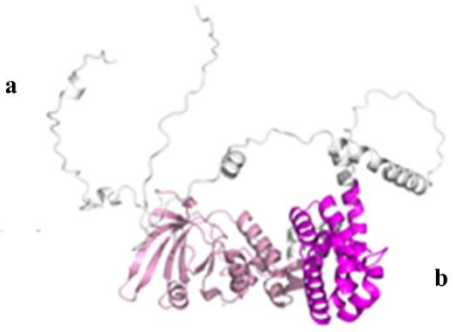


**Fig 2.** ExoT Important Regions (A) ADP Ribosyltransferase (ADPr) domain in light pink (B) GTPase-activating protein (GAP) domain in purple

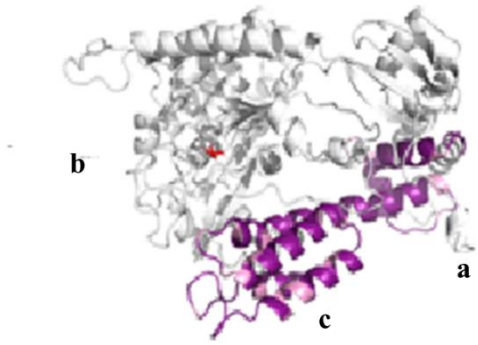


**Fig 4.** ExoU Important Regions (A) patatin-like phospholipase domain in purple (B) catalytic serine residue in red (C) VipD motif in light pink

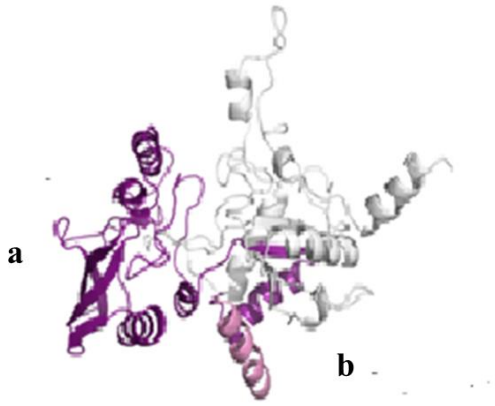


**Fig 5.** ExoY Important Regions (A) catalytic core in purple (B) T3SS signal region in light pink.

**Alignment of the amino acid sequences and phylogenetic tree**

The alignment of amino acid sequences using Clustal Omega revealed several conserved residues and similarities in sequences within the proteins. Notably, ExoS and ExoT displayed a higher degree of sequence similarity (73.29%). In contrast, ExoU and ExoY exhibited greater divergence, with a percentage score of less than 15% with each other and when compared with both ExoS and ExoT.

**Analysis of the secondary structure**

The percentages of secondary structure predictions for T3SS effector proteins (ExoS, ExoT, ExoU, and ExoY) from *Pseudomonas aeruginosa* were analyzed using SOPMA. The predicted secondary structure exhibited that all effector proteins had high percentages of alpha-helices; notably ExoS (66.23%), followed by ExoU (59.10%), and ExoT (58.64%), with the exception of ExoY (27.25%). This is due to ExoY being random coil dominant (57.94%), while ExoU (34.35%), ExoT (33.92%), and ExoS (26.93%) were observed with lower coil percentages. Consequently, all extended strands are in low percentages in all effector proteins with ExoY having the highest percentage (14.81%), then ExoT (7.44%), ExoS (6.84%), and ExoU (6.55%).

**Analysis of the Homology Models**

***Tertiary structure determination, validation, and refinement***

Table 2 presented the initial predicted structures of the target protein, generated through homology modeling using SWISS-MODEL, Phyre2, and I-TASSER, and visualized in PyMOL. Since homology models can have inherent inaccuracies, a thorough validation process was conducted using the SAVES server to ensure structural reliability. This validation primarily focused on the Ramachandran plot analysis, where the percentage of residues residing in the core (Co) regions and the percentage in disallowed regions, served as key metrics for model quality. Models exhibiting a high percentage of residues in the core regions and a low percentage in disallowed regions were considered to have passed the initial validation screening.

Among the models, the SWISS-MODEL-generated structure for ExoS was selected, with 85.6% of its residues in the core regions and 0.5% disallowed regions. SWISS-MODELED structure for ExoT also demonstrated strong model reliability, with 86.6% of residues in the core region and only 0.5% in disallowed regions. Among the modeled structures, ExoU and ExoY demonstrated the highest percentages of residues within the core region (91% and 90%, respectively), with negligible presence of disallowed regions (0% and 0.3%). Although PHYRE2 produced models with higher core region percentages, the SWISS-MODEL structures were selected due to their enhanced structural continuity. The PHYRE2 models exhibited protein breaks that could potentially compromise structural stability and subsequent functional interpretations. The cell wall protein of *A. castellanii* displayed a slightly lower core region percentage of 82.2%, suggesting more flexibility in its structure, possibly due to intrinsically disordered regions or unique structural adaptations. However, the disallowed region was minimal (0.4%).

The SWISS-MODEL structures underwent further refinement using GalaxyWEB to enhance their structural precision. Refined structures were selected based on two primary criteria: (1) the highest percentage of residues within the Ramachandran favored region; and (2) the lowest MolProbity score.

**Tertiary structure evaluation and analysis**

***ExoS and ExoT***

Structural analysis of ExoS revealed a highly structured alpha-helical core, comprising 66.23% alpha-helices. The catalytic domain is located in the C-terminal region (residues 234-453) and is supported by a network of helical bundles. The structure also contains flexible loop regions. ExoT exhibited a similar helical architecture (58.64% alpha-helices) but contained an extended loop region near its active site. The tertiary structure of ExoT supports the presence of both an ADP-ribosyltransferase (ADPRT) domain and a GTPase-activating protein (GAP) domain. Both ExoS and ExoT possess well-defined helical domains. ExoT's structure contains flexible loop regions that may facilitate interactions with host cell components.

***ExoU***

Structural analysis of ExoU revealed a patatin-like phospholipase domain, consisting of 72.39% alpha-helices and 27.61% random coils, with no beta-sheets. The catalytic serine residue is positioned within a deep cleft, and flexible loop regions surround the active site. ExoU also contains a VipD motif, which is structurally positioned to facilitate additional interactions.

***ExoY***

Structural analysis of ExoY revealed that its catalytic domain consists of 32.12% alpha-helices, 25.45% beta-sheets, and 42.42% random coils, indicating a structurally adaptable enzyme. The presence of ATP-binding and metal ion coordination sites contributes to nucleotide interactions and enzymatic stability. Additionally, ExoY contains an N-terminal Type III Secretion System (T3SS) signal region that facilitates its translocation into host cells

**Table 2** Raw Protein Structures from SWISS-MODEL, Phyre2, and i-TASSER.

| | Software | | |
|---|---|---|---|
| | **SWISS-MODEL** | **Phyre2** | **i-TASSER** |
| ExoS (WP_320524392.1) | 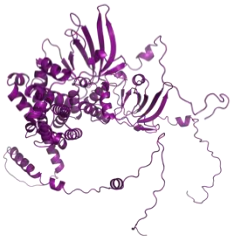 | 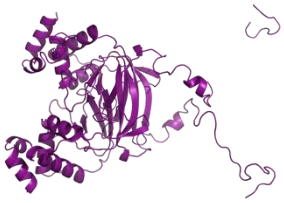 | 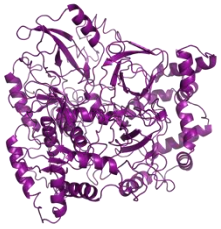 |
| ExoT (WP_039027028.1) | | | |
| ExoU (WP_031686411.1) | 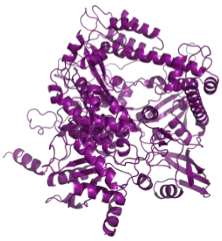 | 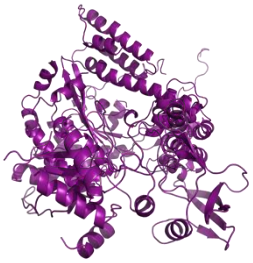 | 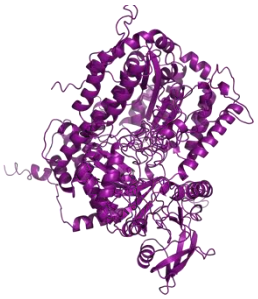 |
| ExoY (WP_319179002.1) | | | |
| Cell wall anchor domain (*A. castellanii* str. Neff) (XP_004338735.1) | 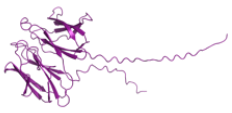 |  | 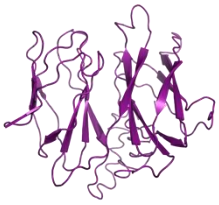 |

**Table 3** Molecular Docking Analysis of the Target Molecules and their Interacting Residues and their Interacting Residues.

| Protein | Target Molecules | Interacting Residues |
|---|---|---|
| ExoS | Receptor | R3 R7 F8 V10 S15 S20 L21 A22 T242 S244 W246 S247 |
| | Ligand | ADPr domain: Y277 R285 R319 G320 R322 G323 G324 R352 S353 Q356 L394<br>Non-domain: D424 P432 E433 S435 Q441 |
| ExoT | Receptor | M1 L2 S5 L6 R7 I11 I13 S15 I57 F58 T59 D60 D68 Y70 W246 |
| | Ligand | GAP-Domain: A112 H214 N218 R224<br>Non-domain: R79 H81<br>ADPr domain: E279 R285 Q289 R291 Q325 R327 D328 E331 T362 R409 |
| ExoU | Receptor | R3 R7 F8 I11 I13 A14 S15 E234 S235 P239 T241 T242 S244 W246 S247 |
| | Ligand | Pat domain: R581 G582 T584 Q586 Q598 D625 V628 R633 E636<br>Non-domain: Y333 E338 W339 E341 V399 G400 K536 |
| ExoY | Receptor | R3 S5 L6 R7 L9 I11 P245 W246 F249 |
| | Ligand | N-Terminal: M26 Q27 D33<br>Catalytic Core Domain: R55<br>Non-domain: R257 E329 |

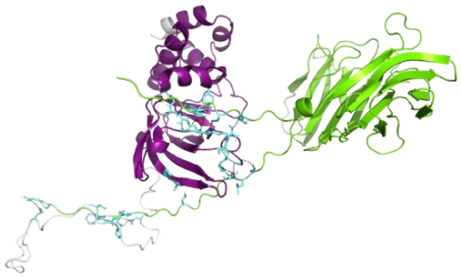

**Fig 6.** ExoS and its interacting residues with *A. castellanii* cell wall. Legend: green – receptor (*A. castellanii* cell wall); purple – ADPr domain; blue – interacting residues; red dashed lines – hydrogen bonds; white – unrelated ligand domains

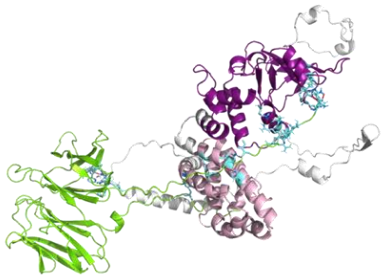

**Fig 7**. ExoT its interacting residues with *A. castellanii* cell wall. Legend: green – receptor (*A. castellanii* cell wall); purple – ADPr domain; pink – GAP domain; blue – interacting residues; red dashed lines – hydrogen bonds; white – unrelated ligand domains

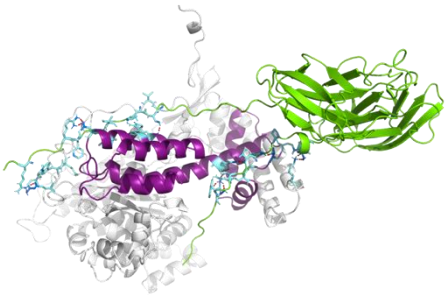

**Fig 8.** ExoU and its interacting residues with *A. castellanii* cell wall Legend: green – receptor (*A. castellanii* cell wall); purple – patatin-like phospholipasedomain; blue – interacting residues; red dashed lines – hydrogen bonds; white – unrelated ligand domains

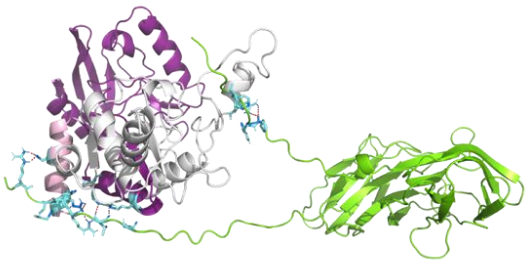

**Fig 9.** ExoY and its interacting residues with *A. castellanii* cell wall. Legend: green – receptor (A. castellanii cell wall); purple – catalytic core domain; blue – interacting residues; red dashed lines – hydrogen bonds; white – unrelated ligand domains

**Molecular Docking Analysis**

The molecular analysis identified specific binding interactions between the T3SS effector proteins and the receptor, cell wall anchor domain of *Acanthamoeba*. Shown in Table 3 are the specific interacting residues for each effector protein and receptor, along with corresponding domains where these interactions took place.

For ExoS, the receptor interacting residues are: R3, R7, F8, V10, S15, S20, L21, A22, T242, S244, W246, and S247. Meanwhile, the ligand interaction seen within the ADPr domain are: Y277, R285, R319, G320, R322, G323, G324, R352, S353, Q356, and L394. Additionally, the non-domain interacting residues are: D424, P432, E433, S435, and Q441.

For ExoT, interacting residues of the receptor are: M1, L2, S5, L6, R7, I11, I13, S15, I57, F58, T59, D60, D68, Y70, and W246. The ligand interacting residues are observed within the GAP domain (A112, H214, N218, and R224), ADPr domain (E279, R285, Q289, R291, Q325, R327, D328, E331, T362, and R409), and non-domain (R79 and H81).

For ExoU, the interacting residues of the receptor are the following: R3, R7, F8, I11, I13, A14, S15, E234, S235, P239, T241, T242, S244, W246, and S247. Ligand interactions were located within the patatin-like phospholipase domain (R581, G582, T584, Q586, Q598, D625, V628, R633, and E636), alongside additional few non-domain interacting residues (Y333, E338, W339, E341, V399, G400, and K536)

For ExoY, the interacting receptor residues are the following: R3, S5, L6, R7, L9, I11, P245, W246, and F249. Ligand interactions were identified to mainly fall within the N-Terminal domain (M26, Q27, D33) and Catalytic core domain (R55). Additionally, non-domain interacting residues R257, and E329 were observed.

**Discussion**

**Structural and Cytotoxic Mechanisms of T3SS Effector Proteins Against *Acanthamoeba***

The molecular characterization of ExoS and ExoT revealed their functional similarities due to their shared ADP-ribosyltransferase (ADPr) domains, which interfere with host cell signaling pathways. However, despite this redundancy, ExoS demonstrated greater hydrophobicity and structural stability, which may enhance its enzymatic activity and interaction with *Acanthamoeba* membranes. The presence of dominant alpha-helices in ExoS contributes to its interaction with cytosolic proteins, potentially facilitating intracellular modification of host signaling pathways (Coburn et al. 2007). Additionally, the higher thermostability of ExoS suggests that it can remain active across varying host conditions, supporting its role in sustained virulence. In contrast, ExoT exhibited a mixed alpha-helix and beta-sheet structure which reflect its dual enzymatic roles in disrupting host defenses. These findings align with Horna & Ruiz (2021), who demonstrated that ExoS and ExoT disrupt actin cytoskeletal dynamics by targeting Rho GTPases, leading to impaired phagocytosis.

Further structural analysis suggests that ExoS is more cytotoxic than ExoT due to its enhanced stability which allows it to persist longer within host cells. Additionally, the differences in their ADPr domain interactions suggest that ExoS may have a broader substrate specificity that enhances its ability to manipulate host signaling pathways. Previous studies on YopE, a Type III effector from *Yersinia* species, have demonstrated a similar ability in disrupting host cytoskeletal dynamics by inactivating Rho GTPases (Wang et al., 2014). However, unlike YopE, ExoS possesses an additional ADPr domain that enhances its cytotoxicity (Reuven et al., 2024), suggesting a more potent role in host cell manipulation.

ExoU was identified as the most cytotoxic effector, possessing phospholipase activity that leads to rapid membrane degradation. Unlike ExoS and ExoT, which primarily disrupt intracellular signaling, ExoU directly targets lipid membranes, causing host cell lysis. Its high hydrophilicity facilitates its rapid integration into host lipid bilayers, reinforcing its role in phospholipid hydrolysis and necrotic cell death. Additionally, ExoU exhibited the highest instability index among the T3SS effector protein indicating a shorter half-life, rapidly degrading after exerting its function. This characteristic aligns with its aggressive and rapid pathogenicity. These findings are consistent with Leong et al. (2022), who reported that ExoU induces rapid necrotic damage in mammalian cells.

Structurally, ExoU has the highest molecular weight among the T3SS effector proteins. This larger size contributes to its ability to accomodate multiple functional domains which enhances its enzymatic activity and interactions with host factors (Fischer et al. 2017). ExoU is composed primarily of alpha-helices, random coils, and the presence of extended strands, with the absence of beta-sheets, suggests an optimized framework for stability and functional flexibility. The limited presence of extended strands contributes to the lower or complete absence of beta-sheets, distinguishing ExoU from other patatin-like phopholipases that rely on beta-sheet support for enzymatic function. Instead, ExoU utilizes its helical structures and dynamic loop regions to achieve efficient phospholipid hydrolysis and membrane disruption. The predominance of alpha-helices provides a stable yet adaptable scaffold that allows ExoU to

undergo conformational changes necessary for efficient membrane targeting and cytotoxic function (Tessmer et al. 2020). Meanwhile, the presence of random coils contributes to its ability to interact with *Acanthamoeba* membranes. The inclusion of extended strands may contribute to substrate binding and enzymatic efficiency.

ExoU's ability to interact with host ubiquitin via its VipD motif adds another layer of its virulence mechanism. This host factor recognition mechanism significantly enhances its enzymatic activity, thereby increasing its cytotoxic potential. Studies have demonstrated that disrupting ExoU's ubiquitin-binding capacity leads to a substantial reduction in pathogenicity (Springer et al. 2019). However, previous studies on ExoU in *P. aeruginosa* lung infections suggest that its activation depends on host ubiquitination pathways (Tessmer et al., 2020). This raises the possibility that ExoU may have a different activation mechanism in *Acanthamoeba.*

ExoY, an adenylate cyclase, has a predominantly random coil structure which increases its flexibility and interaction with host proteins. Its moderate aliphatic index suggests a stable yet adaptable structure that allows it to efficiently function under different conditions. In contrast to ExoS, the negative GRAVY value of ExoS, ExoT, and ExoY indicates its greater affinity for aqueous environments, which supports its role in manipulating intracellular signaling rather than directly targeting membranes (Galán & Waksman, 2018).

ExoY was found to significantly disrupt cytoskeletal integrity by increasing intracellular cAMP levels which could weakens *A. castellanii*'s ability to adhere to surfaces and effectively undergo phagocytosis. This aligns with studies reporting that elevated cAMP concentrations impair host immune responses and cellular architecture (Qin et al., 2022). These findings further demonstrate that ExoY's random coil-dominant structure enhances its conformational flexibility, potentially increasing its ability to interact with various host targets, including *Acanthamoeba* proteins involved in cytoskeletal regulation. Additionally, ExoY's catalytic core domain, which includes key residues such as M26, Q27, and R55 (Table 4), enhances its enzymatic function. The presence of a T3SS signal region within ExoY also ensures efficient translocation into host cells. The identified receptor interactions at R3, S5, and L6, along with ligand binding at M26 and R55, enhance the ability of ExoY to anchor in the host cell's membrane ensuring an efficient enzymatic activity in disrupting cytoskeletal integrity therefore weakening the structural defenses of *A. castellanii.* The instability index of ExoY is lower than ExoT and ExoU, suggesting it maintains stability within host cells, which is crucial for its role in prolonged disruption of host signaling pathways.

Similar to ExoY, the adenylate cyclase toxin CyaA from *Bordetella pertussis* elevates intracellular cAMP, leading to immune cell suppression (Holubova et al., 2021). However, unlike CyaA, which has a built-in calmodulin-binding domain for activation, ExoY relies on host-derived nucleotides, suggesting a distinct mode of regulation (Teixeira-Nunes et al., 2023).

**Molecular Docking of Protein Interactions**

The molecular docking analysis of the T3SS effector proteins revealed their distinct binding interactions with host receptors, particularly the *Acanthamoeba castellanii* cell wall. ExoS demonstrated stable interactions through hydrogen bonds and hydrophobic interactions, particularly within its ADPr domain. These findings align with the study by Kamiski et al. (2018), which emphasized the role of ExoS in modulating host cytoskeletal functions through its enzymatic activity. The identification of interacting residues supports the hypothesis that ExoS plays a critical role in bacterial virulence by modifying host cell signaling pathways.

ExoT exhibited a complex binding profile involving both its GTPase-activating protein (GAP) and ADP-ribosyltransferase domains, forming hydrogen bonds, salt bridges, and hydrophobic interactions with the host receptor. Similar findings were reported by Patil et al. (2010), which highlighted ExoT's dual enzymatic activities in disrupting host cytoskeletal integrity. The presence of these multiple interaction sites suggests that ExoT contributes significantly to pathogenesis, enabling *P. aeruginosa* to impair host immune defenses more effectively. While both ExoS and ExoT disrupt host cellular functions, ExoS is generally considered more cytotoxic due to its stronger enzymatic activity. ExoT, on the other hand, has an additional GAP domain that enhances its ability to interfere with host signaling but is less directly cytotoxic than ExoS.

Furthermore, the results of ExoU molecular docking confirmed that its patatin-like phospholipase (Pat) domain plays a key role in host membrane disruption. This compares to the studies of Springer et al. (2019), which also demonstrated the potential cytotoxic activity of the VIPD motif residues (e.g., Q598, T584, R581) through phospholipid degradation. Unlike ExoS and ExoT, ExoU's mechanism primarily involves direct membrane lysis, leading to rapid cell death. This suggests ExoU takes a more aggressive approach, directly compromising cell viability when compared to ExoS and ExoT, which manipulate host signaling to disrupt function.

Lastly, ExoY formed hydrogen bonds and hydrophobic interactions, particularly at its catalytic core domain, which is responsible for adenylate cyclase activity. The results were similar to the study by Zhang et al. (2024), who noted that ExoY increases intracellular cyclic AMP (cAMP) levels, thereby impairing host cytoskeletal regulation. Compared to ExoS and ExoT, ExoY's virulence strategy appears more indirect, disrupting cellular signaling rather than directly modifying cytoskeletal proteins or lysing membranes. These insights align with previous studies on *P. aeruginosa* virulence but extend our understanding to bacterial-amoebal interactions, supporting the hypothesis that Acanthamoeba serves as an environmental reservoir for *P. aeruginosa*. While the *in silico* docking results provide valuable information into the interactions between the effector proteins and the *Acanthamoeba* cell wall, it is important to acknowledge that these models are based on static protein structures. In biologic systems, however, proteins are dynamic and undergo constant conformational changes. To more accurately reflect these biological conditions, future studies are encouraged to incorporate Molecular Dynamics simulations. This approach would allow for the observation of protein flexibility, binding stability, and structural adaptation over time, which offers a more comprehensive understanding of their cytotoxic mechanisms.

Interestingly, these interactions parallel those of *Legionella pneumophila*, which also exploits *Acanthamoeba* as a host (Ariyadasa et al., 2022). However, while *Legionella* primarily establishes a replicative niche within amoebal vacuoles, *P. aeruginosa* induces cytotoxicity, suggesting distinct survival strategies. Given the rising recognition of bacterial-amoebal symbiosis in opportunistic infections, these findings have implications for microbial ecology, environmental persistence, and pathogen transmission in healthcare and natural settings.

## Conclusion

This study investigated the structural and functional characteristics of the Type III Secretion System (T3SS) effector proteins of *Pseudomonas aeruginosa* and their interactions with *Acanthamoeba castellanii* using an *in silico* approach. The findings highlighted the cytotoxic mechanisms of these effector proteins, particularly ExoU, which exhibited the highest cytotoxic potential due to its phospholipase activity. The study also provided valuable insights into the physicochemical properties of these proteins, including their stability, solubility, and key amino acids involved in their function. Understanding these molecular interactions contributes to a broader knowledge of microbial pathogenesis and its role in amoebic infections. Given the limited efficacy of current treatments against *Acanthamoeba* infections, these findings emphasize the need for further research to explore potential therapeutic applications. Future studies should focus on experimental validation through biochemical assays and co-culture experiments to confirm the *in silico* results. Additionally, these insights could aid in the development of novel anti-amoebic treatments that target specific pathogenic mechanisms, ultimately improving treatment outcomes, particularly for immunocompromised individuals at higher risk of severe infections.

Furthermore, this study provides insights that could support the improvement of water treatment policies and diagnostics for Acanthamoeba infections in the Philippines. It highlights the need for routine protozoan monitoring and use of ultrafiltration treatment as a disinfection method at high-risk areas. Clinically, the underreporting of Acanthamoeba cases may be due to limited diagnostic tools and low awareness of the community. The molecular docking result shows a potential for developing targeted diagnostic markers using the T3SS interactions as a design guide for biomarker-based detection kits. Together, these insights can provide a strong foundation for strengthening public health policies and clinical approaches to mitigate the health risks associated with *Acanthamoeba* infections.

In addition, for the purposes of strengthening the findings of this in silico study, it is suggested that future studies include validation in a laboratory setting. One approach could be designing co-culture systems incorporating *Pseudomonas aeruginosa* and *Acanthamoeba castellanii* being grown together to study how the effector proteins biologically impact the amoeba in real time. With these models, the researchers would be able to directly assess the roles of each T3SS protein: ExoS, ExoT, ExoU, and ExoY, in the destruction and neutralization of the *Acanthamoeba*. Furthermore, wet lab experiments like Gene knockout analysis where certain effector protein genes are silenced, such as exoS, exoT, exoU, or exoY, can illustrate the proteins' unique contributions in neutralizing the *Acanthamoeba*. The assessment of protein activity could be performed to determine the functional activity of the effectors and their interactions with host proteins during infection. Inhibition assays could also be applied to assess whether the blockage of these effector proteins with particular compounds would diminish or eliminate cytotoxic activities directed towards *Acanthamoeba castellani*. These experiments would help in validating the

computational suppositions while reinforcing prospective therapeutic interventions against *Acanthamoeba* infections.

**Acknowledgements**
As aspiring researchers in the field of Medical Technology, this study demanded significant time, effort, and dedication. We are deeply grateful to those who supported and guided us throughout this journey. First and foremost, we thank our loving parents, whose unwavering encouragement and guidance have served as our foundation. Their support has been a constant source of strength and motivation. We also extend our heartfelt appreciation to our batchmate, Hans Olorosisimo, for his generosity in sharing his time and expertise. His willingness to help us understand in silico methods and clarify concepts whenever needed has been truly invaluable. Above all, we offer our deepest gratitude to God Almighty, whose blessings have guided us with strength, wisdom, and perseverance every step of the way.

**Conflict of interest**
The authors declared no potential conflicts of interest with respect to the research, authorship, and/or publication of this article.

**Funding**
The authors received no financial support for the research, authorship, and/or publication of this article.

**Data availability**
All data obtained from this study are included in the current manuscript.

**References**
Ariyadasa S, Billington C, Shaheen M N F, Ashbolt N J, Fee C J, Pang L. (2022). Use of a Novel DNA-Loaded Alginate-Calcium Carbonate Biopolymer Surrogate to Study the Engulfment of *Legionella pneumophila* by *Acanthamoeba* polyphaga in Water Systems. Microbiology Spectrum, 10(4). https://doi.org/10.1128/spectrum.02210-22

Büchele M L C, Nunes B F, Filippin-Monteiro F B, Caumo K S. (2023). Diagnosis and treatment of *Acanthamoeba* Keratitis: A scoping review demonstrating unfavorable outcomes. Contact Lens and Anterior Eye, 46(4), 101844. https://doi.org/10.1016/j.clae.2023.101844

Castro A E, Obusan M C. (2023). Microbial quality and emerging pollutants in freshwater systems of Mega Manila, Philippines: A scoping review. Urban Water Journal, 20(6), 639–651. https://doi.org/10.1080/1573062x.2023.2209559

Chomicz L, Szaflik J, Baltaza W. (2024). *Acanthamoeba* spp. as factors for severe infectious diseases in humans. MDPI. https://doi.org/10.3390/microorganisms12030581

Fischer A, Anderson D M, Tessmer M H, Frank D W, Feix J B, Meiler J. (2017). Structure and Dynamics of Type III Secretion Effector Protein ExoU As determined by SDSL-EPR Spectroscopy in Conjunction with De Novo Protein Folding. 2(6), 2977–2984. https://doi.org/10.1021/ACSOMEGA.7B00349

Galán J E, Waksman G. (2018). Protein injection machines in bacteria. Cell, 172(6), 1306-1318. https://doi.org/10.1016/j.cell.2018.01.034

Holubova J, Juhasz A, Masin J, Stanek O, Jurnecka D, Osickova A, Sebo P, Osicka R. (2021). Selective Enhancement of the Cell-Permeabilizing Activity of Adenylate Cyclase Toxin Does Not Increase Virulence of Bordetella pertussis. International Journal of Molecular Sciences, 22(21), 11655. https://doi.org/10.3390/ijms222111655

Horna, G, Ruiz J. (2021). Type 3 secretion system of *Pseudomonas aeruginosa*. Microbiological Research, 246, 126719. https://doi.org/10.1016/j.micres.2021.126719

Labovská S. (2021). *Pseudomonas aeruginosa* as a Cause of Nosocomial Infections. In *Pseudomonas aeruginosa* - Biofilm Formation, Infections and Treatments. IntechOpen.

Leong, W, Poh W H, Williams J, Lutz C, Hoque M M, Poh Y H., et al. (2022). Adaptation to an amoeba host leads to *Pseudomonas aeruginosa* isolates with attenuated virulence. Applied and Environmental Microbiology, 88(5). https://doi.org/10.1128/aem.02322-21

Li Y, Sun S X. (2023). The influence of polarized membrane ion carriers and extracellular electrical/pH gradients on cell ionic homeostasis and locomotion. bioRxiv. https://doi.org/10.1101/2023.07.26.550658

Milanez G, Masangkay F, Martin I G, Hapan M F, Manahan E, Castillo J, Karanis P. (2022). Epidemiology of free-living amoebae in the Philippines: A review and update. PubMed Central. Retrieved from https://pmc.ncbi.nlm.nih.gov/articles/PMC9387320

Nirjhon R. (2023). BLAST in bioinformatics: Its uses, application & function. Retrieved November 18, 2024, from https://discover.hubpages.com/education/BLAST2

Patil R, Das S, Stanley A, Yadav L, Sudhakar A, Varma A K. (2010). Optimized hydrophobic interactions and hydrogen bonding at the target-ligand interface

leads the pathways of drug designing. PLOS https://doi.org/10.1371/journal.pone.0012029

Qin S, Xiao W, Zhuo C, Pu Q, Deng X, Lan L., et al. (2022). *Pseudomonas aeruginosa*: Pathogenesis, virulence factors, antibiotic resistance, interaction with host, technology advances, and emerging therapeutics. Nature Communications. https://doi.org/10.1038/s41392-022-01056-1

Reuven A D, Mwaura B W, Bliska J. (2024). ExoS Effector in *Pseudomonas aeruginosa* Hyperactive Type III Secretion System Mutant Promotes Enhanced Plasma Membrane Rupture in Neutrophils. bioRxiv. https://doi.org/10.1101/2024.01.24.577040

Scruggs B, Quist T, Zimmerman M B, Salinas J, Greiner M. (2024). Risk factors, management, and outcomes of *Acanthamoeba* keratitis: A retrospective analysis of 110 cases. Science Direct. https://doi.org/10.1016/j.ajoc.2022.101372

So-Young K, Aung J M, Shin M, Moon E-K, Kong H-H, Goo Y-K, Chung D-I, Hong Y. (2022). Sirtinol suppresses trophozoites proliferation and encystation of *Acanthamoeba* via inhibition of sirtuin family protein. *The Korean Journal of Parasitology, 60(1), 1–6.* https://doi.org/10.3347/kjp.2022.60.1.1

Springer T I, Reid T-E, Gies S L, Feix J B. (2019). Interactions of the effector ExoU from *Pseudomonas aeruginosa* with shortchain phosphatidylinositides provide insights into ExoU targeting to host membranes. The Journal of biological chemistry. https://pmc.ncbi.nlm.nih.gov/articles/PMC6916483/

Teixeira-Nunes M, Retailleau P, Raoux-Barbot D, Comisso M, Missinou A A, Velours C., et al. (2023). Functional and structural insights into the multi-step activation and catalytic mechanism of bacterial ExoY nucleotidyl cyclase toxins bound to actin-profilin. bioRxiv. https://doi.org/10.1101/2023.01.13.523968

Tessmer M H, DeCero S A, del Alamo D, Riegert M O, Meiler J, Meiler J, Frank D W, Feix J B. (2020). Characterization of the ExoU activation mechanism using EPR and integrative modeling. Scientific Reports, 10(1), 19700. https://doi.org/10.1038/S41598-020-76023-3

Wang X, Parashar K, Sitaram A, Bliska J B. (2014). The GAP activity of type III effector YopE triggers killing of *Yersinia* in macrophages. PLOS Pathogens, 10(8). https://doi.org/10.1371/JOURNAL.PPAT.1004346

Wang Y, Jiang L, Zhao Y, Ju X, Wang L, Jin L, Fine R D, Li M. (2023). Biological characteristics and pathogenicity of acanthamoeba. *Frontiers in Microbiology*, *14*. https://doi.org/10.3389/fmicb.2023.1147077

Zhang X, Yu C-X, Song L-J (2024). Progress on the Regulation of the Host Immune Response by Parasite-Derived Exosomes. Pathogens, 13(8), 623. https://doi.org/10.3390/pathogens13080623